

# Nonlinear Duopoly Games with Advertisement\*

Akio Matsumoto<sup>†</sup>

Department of Economics  
Chuo University  
Hachioji, Tokyo, 192-0393, JAPAN

Ferenc Szidarovszky<sup>‡</sup>

Department of Systems and Industrial Engineering  
University of Arizona  
Tucson, Arizona, 85721-0020, USA

June 22, 2007

## Abstract

This study introduces advertisement into the dynamic nonlinear duopoly model. It demonstrates three major findings. The first is that the model can be destabilized via either flip bifurcation or Hopf bifurcation, the second is that a half-pitchfork bifurcation of output occurs when the advertisement dynamics is periodic and the nonlinearity of the output dynamics becomes stronger, and the third is that the existence of attractor and the coexistence of attracting sets are the main features of the model when it is locally unstable.

---

\*We highly appreciate financial supports from the Japan Ministry of Education, Culture, Sports, Science and Technology (Grant-in-Aid for Scientific Research (A) 16203019) and the US Air Force Office of Scientific Research (MURI grant N14-03-1-150). We are also grateful to J. Minagawa for his supporting computational studies.

<sup>†</sup>742-1, Higashi-Nakano, Hachioji, Tokyo, 192-0393, Japan. akiom@tamacc.chuo-u.ac.jp; +81-426-74-3551 (tel); +81-426-74-3425 (fax).

<sup>‡</sup>Tucson, AZ, 85721-0020, USA. szidar@sie.arizona.edu; +01-520-621-6557 (tel); +01-520-621-6555 (fax).

# 1 Introduction

In the recent literature, several authors have demonstrated that nonlinear oligopoly competition may be chaotic. Rand (1978) considers duopoly chaos from the mathematical point of view, Puu (1991) and Kopel (1996) examine duopoly chaos from the economic point of view, Puu and Sushko (2002) and Bischi, Chiarella, Kopel and Szidarovszky (2008) give a comprehensive summary of recent developments in nonlinear oligopoly theory. These works indicate that dynamic nonlinear oligopoly models may explain various complex behavior observed in real economy. It has been well-known that advertisement is one of the most important activities in economy. Since the publication of the seminal paper of Nerlove and Arrow (1962), many studies have been devoted to determine optimal advertising expenditures over time in the dynamic optimal control framework in which the goodwill of the firm is the stock variable and the advertisement expenditure is the flow variable. See Sethi (1977) and Feichtinger, Hartl and Sethi (1994) for comprehensive survey of the literature on advertisement policy. In the existing literature, the authors have ignored the advertisement effects on oligopoly competition. The only exception is Ahmad, Agiza and Hassan (1999) (AAH, henceforth) who have studied advertisement in Cournot duopoly models and consider chaos control by applying OGY method. In spite of their efforts, it has not yet been fully known how advertisement affects the nonlinear oligopoly competition.

The main purpose of this paper is to provide a possible and positive answer to this question. For this purpose, we use the dynamic model of AAH and present a constructive method to derive stationary state outputs in terms of model's parameters. With this explicit form of the stationary state, we can provide the explicit forms of local stability conditions and, with this condition, we can proceed to global dynamics in the case of local unstable stationary points. Another interesting finding of this paper is that the dynamic system shows a *half-pitchfork bifurcation* on the way to chaos: at the bifurcation points, only half of the periodic points gives birth of period-doubling points.

This paper is organized as follows. Section 2 introduces the dynamic model and determines its stationary state. Section 3 discusses the local dynamics and derives the stability condition on which our main study is based. Section 4 examines global dynamics under homogenous advertisement strategy in which the two firms adopt the same strategy and under the heterogeneous advertisement strategy in which the two firms adopt different strategies. Section 5 makes concluding remarks.

## 2 4D Model

We reconsider the nonlinear dynamic duopoly model with advertisement introduced by AAH:

$$\begin{aligned}
 q_1(t+1) &= (1 + x_1(t)) \left( \sqrt{\frac{q_2(t)}{c_1}} - q_2(t) \right), \\
 q_2(t+1) &= (1 + x_2(t)) \left( \sqrt{\frac{q_1(t)}{c_2}} - q_1(t) \right), \\
 x_1(t+1) &= (1 - r_1)x_1(t) + a_1x_1(t)(1 - x_1(t)) - b_1x_1(t)x_2(t), \\
 x_2(t+1) &= (1 - r_2)x_2(t) + a_2x_2(t)(1 - x_2(t)) - b_2x_1(t)x_2(t).
 \end{aligned} \tag{1}$$

Here  $r_i$  represents a positive depreciation rate which is assumed to be less than unity,  $a_i$  is a positive constant representing advertisement outlay,  $b_i$  is a positive constant showing the effect of the competition on the advertisement of both firms,  $c_i$  is a positive constant giving the marginal cost of production,  $x_i$  is the goodwill representing the effects of current and past advertising outlays and  $q_i$  is the output produced. Dynamics is considered in discrete time that is denoted by  $t$ . The whole model is divided into two submodels. The first two equations construct a dynamic model of output with advertisement  $x_i$ , which is a variant of the nonlinear duopoly model studies earlier by Puu (2003). The last two equations represent a dynamic model of the advertisement, which is based on the nonlinear models for advertisement introduced by Luhta and Virtanen (1996). It can be seen that the advertisement model affects output dynamics via oscillations of  $x_i$  but not *vice versa*.

### 2.1 Advertisement Model

The advertisement equations incorporate three different effects: the depreciation effect, denoted by  $r_i$ , shows that the goodwill contributes less on demand as time goes on; the nonlinear second term indicates that the advertising outlays increase the goodwill when its level is relatively small and decrease it when the level becomes larger than the threshold; and the interdependency effect is given by the third term. In this study, for the sake of simplicity, we pay our attentions to the first two effects on output dynamics and defer the discussion on the third effect by making the following assumption,<sup>1</sup>

**Assumption 1**  $b_1 = b_2 = 0$ .

---

<sup>1</sup>A more general model with positive  $b_i$  will be considered in a subsequent paper.

As a consequence of this assumption, the advertisement model becomes a system of two independent equations and thus its dynamics becomes uncoupled. Furthermore, to simplify the exposition, let us denote the right hand sides of the last two equations in (1) by  $\varphi_1(x_1)$  and  $\varphi_2(x_2)$ . Then the advertisement model can be rewritten as

$$\begin{aligned}x'_1 &= \varphi_1(x_1), \\x'_2 &= \varphi_2(x_2),\end{aligned}\tag{2}$$

where  $'$  denotes the unit-time advancement operator. Solving  $x'_i = x_i$  provides the fixed point,  $x_i^e$ , of the advertisement model:

$$x_1^e = 1 - \frac{r_1}{a_1} \text{ and } x_2^e = 1 - \frac{r_2}{a_2}.$$

To make these fixed points economically feasible, we assume

**Assumption 2**  $r_i < a_i$  for  $i = 1, 2$ .

Under Assumption 1, the advertisement model becomes, the so called, *folded handkerchief map* in which  $\varphi_i(x_i)$  is a unimodal map being topologically conjugated to the logistic map. Dynamic characteristic of this map is now well-known. It generates rich dynamics ranging from periodic cycles to chaotic behavior. In order to guarantee the feasibility (i.e., nonnegativity and boundness) of the trajectories generated by the advertisement model, we need to introduce a confinement condition. The advertisement model is subject to the non-negativity constraint if

$$0 \leq x_i \leq \frac{1 + a_i - r_i}{a_i}.$$

Solving  $\frac{d\varphi_i}{dx_i} = 0$  gives the maximizer,

$$x_i^m = \frac{1 + a_i - r_i}{2a_i},$$

and the maximum value of  $x_i$ :

$$\varphi(x_i^m) = \frac{(1 + a_i - r_i)^2}{4a_i}.$$

Given  $a_i$  and  $r_i$ , a trajectory  $x_i$  stays within this feasible region for all  $t$  if the maximum value is transformed into the non-negative region:

$$\frac{(1 + a_i - r_i)^2}{4a_i} \leq \frac{1 + a_i - r_i}{a_i},$$

which implies the following confinement condition for  $x_i$ :

**Assumption 3**  $a_i - r_i \leq 3$  for  $i = 1, 2$ .

Due to Assumptions 2 and 3, the feasible set of  $(a_1, a_2)$  is defined as

$$A = \{(a_1, a_2) \mid r_i < a_i \leq 3 + r_i \text{ for } i, j = 1, 2.\}.$$

## 2.2 Output model

Assuming that the inverse demand function is isoelastic and the production costs are linear, Puu (2003) constructs nonlinear duopoly and triopoly models and shows that these models can be chaotic if nonlinearities involved become stronger. In (1), advertisement effects are introduced into Puu's duopoly model in which two competitors, firm 1 and firm 2, produce non-differentiated good of quantities  $q_1$  and  $q_2$  with linear production costs, where the marginal costs are  $c_1$  and  $c_2$ , respectively. Following the traditional spirit of the classical Nerlove-Arrow optimal advertisement model, we assume that each firm has its own goodwill and can sell more product if it has better goodwill. One simple way to incorporate the effects of the goodwill is to assume the following form of the inverse demand function that firm  $i$  perceives,

$$p_i = \frac{1}{\frac{q_i}{1+x_i} + q_j}$$

in which  $x_i \geq 0$  denotes the advertisement effect or the value of the goodwill.  $x_i = 0$  implies no advertisement effects and thus the two goods becomes identical. When  $x_i > 0$ , firm  $i$  can sell larger quantity due to the positive advertisement effects, taking the competitor's output  $q_j$  and market price given. Thus the profit of firm  $i$  is given as

$$\pi_i = \frac{q_i}{\frac{q_i}{1+x_i} + q_j} - c_i q_i$$

which is maximized with respect to  $q_i$ . Using the first-order condition, we can solve for the reaction function,

$$q_i = (1+x_i) \left( \sqrt{\frac{q_j}{c_i}} - q_j \right) \text{ for } i = 1, 2.$$

These considerations provide a microeconomic interpretation of the reaction functions assumed in (1).

To simplify the exposition, again, let us denote the right hand sides of the first two equations of (1) by  $\phi_1(q_2, x_1)$  and  $\phi_2(q_1, x_2)$ . Then the output model can be rewritten as

$$\begin{aligned} q_1' &= \phi_1(q_2, x_1), \\ q_2' &= \phi_2(q_1, x_2). \end{aligned} \tag{3}$$

For  $x_i = 0$ , the output dynamic model is reduced to the nonlinear duopoly model of Puu (2003) in which complex dynamics can be generated, depending on the production cost ratio. Indeed it has been shown that the stationary point of Puu's model is asymptotically stable if and only if the cost ratio belongs to the interval  $(\frac{1}{3+2\sqrt{2}}, 3+2\sqrt{2})$ . It is unstable otherwise, but goes through period-doubling bifurcation to chaos if the ratio decreases from  $\frac{1}{3+2\sqrt{2}}$  to  $\frac{4}{25}$  or increases from  $3+2\sqrt{2}$  to  $\frac{25}{4}$ . Furthermore, it is numerically established that the dynamics is symmetric with respect to unit value of the marginal cost ratio. Thus it is safe to assume that the ratio is greater than unity:

**Assumption 4**  $c_2 \geq c_1$ .

In order to obtain the fixed points of  $q_1$  and  $q_2$  in (3), we set  $q_i' = q_i$ , assume that the fixed point  $(x_1^e, x_2^e)$  of the advertisement dynamics is given and then rewrite the output dynamics as

$$\begin{aligned} q_1 + (1 + x_1^e)q_2 &= (1 + x_1^e)\sqrt{\frac{q_2}{c_1}}, \\ q_2 + (1 + x_2^e)q_1 &= (1 + x_2^e)\sqrt{\frac{q_1}{c_2}}. \end{aligned} \tag{4}$$

Squaring both sides of these equations, dividing the resulting first equation by the second one and introducing the new variables

$$z = \frac{q_2}{q_1}, \quad c = \frac{c_2}{c_1}, \quad d_1 = 1 + x_1^e \text{ and } d_2 = 1 + x_2^e,$$

we obtain the following relation

$$cz = \left( \frac{d_2(1 + d_1z)}{d_1(d_2 + z)} \right)^2. \tag{5}$$

This is a cubic equation for unknown  $z$ . Although it is possible to derive an explicit form of the real root of (5), the form has a very complicated

expression which is not useful for the following analysis. Thus, instead of solving the equation, we look for the intersection of the right and left hand sides of (5) which determines the fixed point of the output ratio.

Let us denote the left hand side by  $f(z)$  and the right hand side by  $g(z)$ :

$$f(z) = cz \text{ and } g(z) = \left( \frac{d_2}{d_1} \frac{1 + d_1 z}{d_2 + z} \right)^2.$$

It can be seen that  $g(z)$  has upper and lower bounds and is positive-sloping,

$$g(0) = \frac{1}{(d_1)^2} < 1,$$

$$\lim_{z \rightarrow \infty} g(z) = (d_2)^2 > 1,$$

and

$$g'(z) = 2 \left( \frac{d_2}{d_1} \right)^2 \frac{(1 + d_1 z)(d_1 d_2 - 1)}{(d_2 + z)^3} > 0.$$

Clearly,  $f(z)$  is strictly increasing, linear and  $f(0) = 0$ . An examination of the solution formula of the cubic equations shows that there is a unique positive intersection  $\alpha$  of  $f(z)$  and  $g(z)$  if  $1 < d_i < 2$ . It corresponds to the real root of the cubic equation and determines the ratio of outputs at the intersection:

$$\alpha = \alpha(c, d_1, d_2) = \frac{q_2^e}{q_1^e},$$

where  $q_i^e$  is the stationary output of firm  $i$ .

Figure 1 gives the graphical representation of the stationary output ratio, in which two graphs of  $f(z)$  with  $c_A = 1.15$  and  $c_B = 1.5$ , two graphs of  $g(z)$  with  $(\frac{r_1}{a_1}, \frac{r_2}{a_2}) = (0.6, 0.2)$  denoted by  $g_I(x)$  and with  $(\frac{r_1}{a_1}, \frac{r_2}{a_2}) = (0.2, 0.6)$  denoted by  $g_{II}(x)$  are shown. There are four intersections,  $A, B, a, b$  of these functions as illustrated. This figure reveals two issues: first, the ratio of outputs can be larger than unity even under Assumption 4 and second, the effect on the output ratio caused by a change in  $c$  is negative. To check the first issue, we consider  $g(z)$  at  $z = 1$  which, after arranging terms, is given by

$$g(1) = \left\{ \frac{\left(2 - \frac{r_2}{a_2}\right)\left(3 - \frac{r_1}{a_1}\right)}{\left(2 - \frac{r_1}{a_1}\right)\left(3 - \frac{r_2}{a_2}\right)} \right\}^2.$$

It is obvious that the ratio  $\alpha$  is less than unity if  $g(1) \leq c$  because the intersection of  $f(z)$  and  $g(z)$  surely occurs in the interval  $(0, 1)$  as shown

by points  $B, a$  and  $b$ , and that it is greater than unity if  $g(1) > c$  as given by point  $A$ .<sup>2</sup> It is also shown that  $g(1) \leq 1$  if  $\frac{r_1}{a_1} \leq \frac{r_2}{a_2}$  and  $g(1) > 1$  if  $\frac{r_1}{a_1} > \frac{r_2}{a_2}$  in which case  $g(1) > c$  could be possible. The second issue is clear as the intersection moves to  $B$  from  $A$  or to  $b$  from  $a$ , respectively, when the marginal cost ratio increases from  $c_A$  to  $c_B$ . These results are summarized in the following theorem:

**Theorem 1** (1) If  $\frac{r_1}{a_1} \leq \frac{r_2}{a_2}$  or if  $\frac{r_1}{a_1} > \frac{r_2}{a_2}$  and  $c \geq g(1)$ , then  $\alpha \leq 1$ ; (2) If  $\frac{r_1}{a_1} > \frac{r_2}{a_2}$  and  $c < g(1)$ , then  $\alpha > 1$ , and (3)  $\frac{d\alpha}{dc} < 0$ .

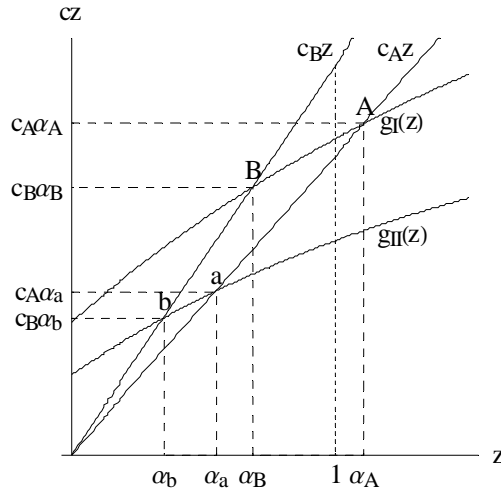


Figure 1. Determinations of the output ratio

Substituting  $q_1^e = \alpha q_2^e$  into the first and second equations of (4) and solving each equation for  $q_i$  provides the stationary values of the outputs in terms of parameters  $a_i$ ,  $c_i$  and  $r_i$ ,

$$\begin{aligned} q_1^e &= \frac{\alpha}{c_1} \left( \frac{d_1}{1 + \alpha d_1} \right)^2 = \frac{1}{c_2} \left( \frac{d_2}{\alpha + d_2} \right)^2, \\ q_2^e &= \frac{1}{c_1} \left( \frac{\alpha d_1}{1 + \alpha d_1} \right)^2 = \frac{\alpha}{c_2} \left( \frac{d_2}{\alpha + d_2} \right)^2. \end{aligned} \tag{6}$$

<sup>2</sup> $g(1)$  takes the maximum value,  $(\frac{4}{3})^2$ , when  $\frac{r_1}{a_1} = 1$  and  $\frac{r_2}{a_2} = 0$ . Therefore,  $\alpha < 1$  always if the marginal cost ratio  $c$  is larger than this maximum value.

Since  $\alpha$  is the real root of the cubic equation (5), it is difficult and complicated to analytically derive the effects on the stationary outputs caused by changes in parameter values but numerical investigations indicate that for firm 1,

$$\frac{\partial q_1^e}{\partial(\frac{r_1}{a_1})} < 0, \quad \frac{\partial q_1^e}{\partial(\frac{r_2}{a_2})} < 0, \quad \frac{\partial q_1^e}{\partial c} < 0,$$

and for firm 2,

$$\frac{\partial q_2^e}{\partial(\frac{r_1}{a_1})} > 0, \quad \frac{\partial q_2^e}{\partial(\frac{r_2}{a_2})} < 0, \quad \frac{\partial q_2^e}{\partial c} < 0.$$

Negative derivatives of  $q_1^e$ ,  $q_2^e$  and  $\alpha$  with respect to  $c$  imply that the elasticity of  $q_2^e$  with respect to  $c$  is larger in absolute value than the elasticity of  $q_1^e$ ,

$$\frac{\partial \alpha}{\partial c} = \frac{\alpha}{c} \left\{ \frac{c}{q_2^e} \frac{\partial q_2^e}{\partial c} - \frac{c}{q_1^e} \frac{\partial q_1^e}{\partial c} \right\} < 0 \Rightarrow \left| \frac{c}{q_2^e} \frac{\partial q_2^e}{\partial c} \right| < \left| \frac{c}{q_1^e} \frac{\partial q_1^e}{\partial c} \right|.$$

As in the case of the advertisement dynamics, in order to avoid negative output values, we need a confinement condition for the output. To this end, we first derive the domain of the output generating function  $\phi_i(q_j, x_i)$  of firm  $i$

$$0 \leq q_j \leq \frac{1}{c_i},$$

and then look for the condition for which the output stays in this domain for all  $t$ . It is seen that  $\phi_i(q_j, x_i)$  has a mound-shaped curve and takes its maximum value

$$q_i^{\max} = \frac{1 + x_i}{4c_i}$$

at  $q_j^m = \frac{1}{4c_i}$ . The output trajectory stays within the feasible region if  $\phi_1(q_2^{\max}) \leq \frac{1}{c_2}$  and  $\phi_2(q_1^{\max}) \leq \frac{1}{c_1}$ . After arranging the terms, these conditions can be rewritten as

$$\frac{4(1 + x_1)(1 + x_2)^2}{(4 + (1 + x_1)(1 + x_2))^2} \leq c \leq \frac{(4 + (1 + x_1)(1 + x_2))^2}{4(1 + x_1)^2(1 + x_2)}.$$

For  $0 \leq x_1 < 3$  and  $0 \leq x_2 < 3$ , the left hand side becomes strictly less than unity and the right hand side becomes strictly greater than unity. As mentioned above,  $x_i$  has its upper bound,  $\frac{1+a_i-r_i}{a_i}$ , below 3 if  $a_i \geq 0.5$ . The confinement condition needs to be taken into account when the stationary state is unstable. As it will be shown later,  $a_i$  is larger than  $2 + r_i$  when the stationary state is unstable. This observation and Assumption 4 (i.e.,  $c \geq 1$ ) imply that the lower bound confinement condition on  $c$  is redundant. Thus we rewrite the confinement condition of the output as follows:

$$c \leq \psi(x_1, x_2), \tag{7}$$

where

$$\psi(x_1, x_2) = \frac{(4 + (1 + x_1)(1 + x_2))^2}{4(1 + x_1)^2(1 + x_2)}. \quad (8)$$

### 3 Local Stability

We next consider the local stability of the 4D dynamic system (1). The Jacobian of the system at the fixed point reads

$$J = \begin{pmatrix} 0 & J_{12} & J_{13} & 0 \\ J_{21} & 0 & 0 & J_{41} \\ 0 & 0 & J_{33} & 0 \\ 0 & 0 & 0 & J_{44} \end{pmatrix},$$

where

$$\begin{aligned} J_{12} &= d_1 \left( \frac{1}{2\sqrt{c_1 q_2^e}} - 1 \right), & J_{13} &= \frac{q_1^e}{d_1}, \\ J_{21} &= d_2 \left( \frac{1}{2\sqrt{c_2 q_1^e}} - 1 \right), & J_{24} &= \frac{q_2^e}{d_2}, \\ J_{33} &= 1 - (a_1 - r_1), & \text{and } J_{44} &= 1 - (a_2 - r_2). \end{aligned}$$

Its characteristic equation has the factored form

$$(\lambda^2 - J_{12}J_{21})(\lambda - J_{33})(\lambda - J_{44}) = 0.$$

Denote by  $\lambda_{1,2}$  the roots of the first factor and by  $\lambda_3$  and  $\lambda_4$  the roots of the second and third factors, respectively. The four roots are

$$\begin{aligned} \lambda_1 &= \sqrt{d_1 d_2 \left( \frac{1}{2\sqrt{c_1 q_2^e}} - 1 \right) \left( \frac{1}{2\sqrt{c_2 q_1^e}} - 1 \right)}, \\ \lambda_2 &= -\lambda_1, \\ \lambda_3 &= 1 - (a_1 - r_1) < 1, \\ \lambda_4 &= 1 - (a_2 - r_2) < 1. \end{aligned}$$

The 4D dynamic system is locally asymptotically stable if all roots are inside the unit circle of the complex plane.

Clearly  $\lambda_3$  and  $\lambda_4$  are the eigenvalues of the advertisement model and they are less than unity due to Assumption 3, implying that the slope of the corresponding advertisement function evaluated at the fixed point is less than unity. Thus if the slope is greater than  $-1$ , then the advertisement model is stable. It is obvious that  $|\lambda_i| < 1$  if  $a_i < 2 + r_i$  and  $|\lambda_i| > 1$  if  $a_i > 2 + r_i$ . Consequently, we obtain the following result.

**Lemma 1** *The advertisement fixed point  $(x_1^e, x_2^e)$  is locally asymptotically stable if  $r_1 < a_1 < 2 + r_1$  and  $r_2 < a_2 < 2 + r_2$ .*

The flip boundary is  $a_i = 2 + r_i$  on which  $\lambda_i$  is equal to  $-1$  and thus a loss of stability just occurs. As the parameter  $a_i$  crosses this boundary and increases further, a solution of the advertisement dynamic system goes through a period doubling cascade to chaos, the most common route to chaos.

We now turn our attentions to the stability of the output dynamics. From (6), we have

$$c_1 q_2^e = \left( \frac{d_2}{\alpha + d_2} \right)^2$$

and

$$c_2 q_1^e = \left( \frac{\alpha d_1}{1 + \alpha d_1} \right)^2,$$

both of which are substituted into the right hand side of  $\lambda_1$  to obtain

$$\lambda_1 (= -\lambda_2) = \frac{1}{2} \sqrt{(\alpha^{-1} - d_1)(\alpha - d_2)}.$$

Denoting  $d_m = \min(d_1, d_2)$  and noticing that  $0 < d_i < 2$ , the expression under the square root is negative, since

$$\begin{aligned} (\alpha^{-1} - d_1)(\alpha - d_2) &= d_1 d_2 - (\alpha d_1 + \alpha^{-1} d_2) \\ &< d_1 d_2 - (\alpha + \alpha^{-1}) d_m \\ &< d_1 d_2 - 2 d_m < 0. \end{aligned}$$

Thus  $\lambda_1$  and  $\lambda_2$  are pure imaginary roots.  $(\alpha^{-1} - d_1)(\alpha - d_2) = -4$  is the Hopf boundary on which the absolute values of the eigenvalues become unity. Hence, we obtain the following result.

**Lemma 2** *The fixed point  $(q_1^e, q_2^e)$  of the output model is locally asymptotically stable if  $(\alpha^{-1} - d_1)(\alpha - d_2) > -4$ .*

From Lemma 1 and 2, the stability conditions of the 4D dynamic system are summarized in the following way.

**Theorem 2** *The 4D dynamic system (1) is locally asymptotically stable if  $r_1 < a_1 < 2 + r_1$ ,  $r_2 < a_2 < 2 + r_2$  and  $(\alpha^{-1} - d_1)(\alpha - d_2) > -4$  where  $d_i = 2 - \frac{r_i}{a_i}$  and  $\alpha$  is the real solution of the cubic equation,*

$$c\alpha = \left( \frac{d_2}{d_1} \frac{1 + d_1 \alpha}{d_2 + \alpha} \right)^2.$$

## 4 Global Behavior

If any one or more of the local stability conditions is violated, then a trajectory soon or later moves away from the fixed point. However, nonlinearities of the model prevent the trajectory from globally diverging. As a consequence, the trajectory neither converges nor diverges but keeps oscillating around the fixed point. Indeed, if the trajectory crosses either the flip boundary or the Hopf boundary, it exhibits various dynamics ranging from simple periodic behavior to complex dynamics involving chaos. We will study such global dynamics in this section. We will assume first that the firms adopt the homogeneous advertisement strategy in which  $r_i = r$  and  $a_i = a$  as a benchmark case in Section 4.1, and then we will proceed to the heterogeneous advertisement case in Section 4.2 in which  $r_1 \neq r_2$  and/or  $a_1 \neq a_2$ .

### 4.1 Homogeneous Advertisement

We consider now the homogeneous case in which each firm has the same depreciation rate and the same advertisement outlay,  $r_1 = r_2 = r$  and  $a_1 = a_2 = a$ . The advertisement equations become identical in the sense that time evolutions of two firms' advertisements behave identically over time if the same initial conditions are chosen. By this simplifying assumption, we can write  $\varphi_1 = \varphi_2 = \varphi$  and call  $\varphi$  the advertisement map. The 4D dynamic system is now written as

$$\begin{aligned} q'_i &= \phi_i(q_j, x_i), \\ x'_i &= \varphi(x_i) \text{ for } i, j = 1, 2 \text{ and } i \neq j. \end{aligned} \tag{9}$$

The analysis of the dynamic behavior of this system is further divided into three parts. First, the basin structures of the advertisement model and their effect on the output dynamics is studied. Second, we restrict (9) to the diagonal of the  $(x_1, x_2)$  space and characterize the output dynamics here, and finally, we study the *half-pitchfork* bifurcation structure of the restricted system, which means that at a bifurcation point, only a half of the periodic points divides into two periodic points with period-doubling and the other half of the periodic points does not.

#### 4.1.1 Homogenous 4D Model

The stationary point of (9) in the homogenous case is the following:

$$q_1^e = \frac{1}{c_2} \left( \frac{d}{\alpha + d} \right)^2, \quad q_2^e = \frac{1}{c_1} \left( \frac{\alpha d}{1 + \alpha d} \right)^2 \quad \text{and} \quad x^e = 1 - \frac{r}{a},$$

where  $x^e = x_1^e = x_2^e$ ,  $d = 1 + x^e$  and  $\alpha = \alpha(c, d, d)$ . The advertisement dynamics is described by the double logistic map. It is well-known that each logistic map  $\varphi(x_i)$  goes to chaos through period-doubling cascade; the stationary state is attracting for  $a < r + 2$ , the stationary state becomes repelling and an attracting period-2 cycle appears for  $r + 2 < a < r + \sqrt{6}$ , the period-2 cycle becomes repelling and an attracting period-4 cycle appears for  $r + \sqrt{6} < a < r + 2.54409$ , and so on. Cycles with odd period can also be found: the onset of the period-3 cycle is at  $a = r + 2\sqrt{2}$ , the onset for period-5 is  $a = r + 2.73817$ , and so forth. Accordingly, one of the main features of the double logistic map is the birth of complicated dynamics and the other is the coexistence of periodic cycles. We investigate the basin structures to capture the latter feature.

In the period-2 region with  $a = 3$  and  $r = 0.6$ , each  $\varphi(x_i)$  has two period-2 points  $x_i^A$  and  $x_i^B$  such that  $x_i^A = \varphi(x_i^B)$  and  $x_i^B = \varphi(x_i^A)$ . Thus the double logistic map has four points of the  $(x_1, x_2)$  plane that form two period-2 cycles;  $A = (x_1^A, x_2^A) \leftrightarrow B = (x_1^B, x_2^B)$  on the diagonal and  $a = (x_1^A, x_2^B) \leftrightarrow b = (x_1^B, x_2^A)$  on the off-diagonal.<sup>3</sup> To avoid the emergence of complicated dynamics, we consider the case in which the output model is stable if the goodwill (that is,  $x_i$ ) is constant. By doing so, we can see which kind of dynamics is produced by the logistic map and how the advertisement dynamics affects the output dynamics. Since it has two periodic cycles, the double logistic map has two basins of attractions as shown in Figure 2A in which the red regions form the basin of the diagonal attractor and the light blue regions represent the basin of the off-diagonal attractor. The advertisement dynamics is path-dependent, so it depends on the choice of the initial point which cycle it eventually converges to. Since the output dynamics depends on the advertisement dynamics, it exhibits periodic oscillations with period-2 if the advertisement dynamics gives rise to a period-2 cycle. In the case when the advertisement dynamics starts at either point  $A$  or  $B$  of the advertisement space in Figure 2A, the output trajectory converges to the period-2 cycle moving between points  $A$  and  $B$  of the output space in Figure 2B. Similarly, if point  $a$  or  $b$  is selected as the initial point, then the output trajectory converges to the other period-2 cycle oscillating between points  $a$  and  $b$  shown in Figure 2B. Note that these output cycles do not coexist while two advertisement cycles do. It depends on the initial point selection of the advertisement map which cycle the output trajectory is periodic to.

---

<sup>3</sup>Since  $x_i = 0$  is also a fixed point of  $\varphi_i$ , we have two more period-2 cycles that periodically visit points on the horizontal or vertical axis of the  $(x_1, x_2)$  plane as one of the periodic points is zero. We do not consider this kind of cycles in the following analysis.

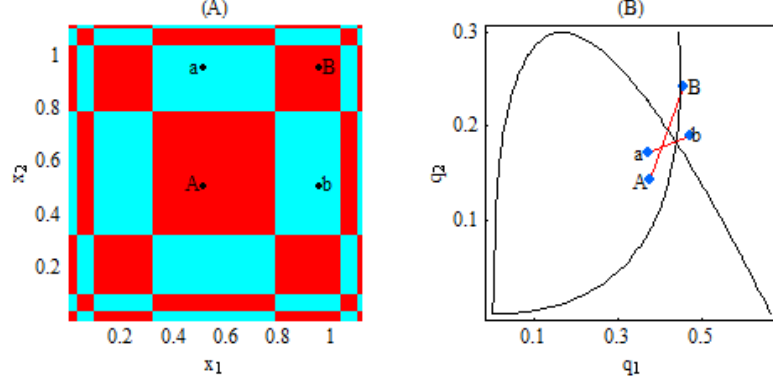


Figure 2. Two basins of attractors with  $a = 3$  and corresponding period-2 cycles

In the period-4 region with  $a = 3.14$  and  $r = 0.6$ , each  $\varphi(x_i)$  has four period-4 points  $x_i^k$  such that  $x_i^k = \varphi^A(x_i^k)$  for  $i = 1, 2$  and  $k = A, B, C, D$  thus the double logistic map has the following coexisting four period-4 cycles:

$$\begin{aligned}
 (x_1^A, x_2^A) &\Rightarrow (x_1^B, x_2^B) \Rightarrow (x_1^C, x_2^C) \Rightarrow (x_1^D, x_2^D) \Rightarrow (x_1^A, x_2^A), \\
 (x_1^A, x_2^B) &\Rightarrow (x_1^B, x_2^C) \Rightarrow (x_1^C, x_2^D) \Rightarrow (x_1^D, x_2^A) \Rightarrow (x_1^A, x_2^B), \\
 (x_1^A, x_2^C) &\Rightarrow (x_1^B, x_2^D) \Rightarrow (x_1^C, x_2^A) \Rightarrow (x_1^D, x_2^B) \Rightarrow (x_1^A, x_2^C), \\
 (x_1^A, x_2^D) &\Rightarrow (x_1^B, x_2^A) \Rightarrow (x_1^C, x_2^B) \Rightarrow (x_1^D, x_2^C) \Rightarrow (x_1^A, x_2^D),
 \end{aligned}$$

in which the first cycle moves in the diagonal and the other three in the off-diagonal. The basin of attractor in the period-4 regions is shown in Figure 3A. For the sake of simplicity, we do not depict periodic points in Figure 3A and illustrate only a period-4 cycle that corresponds to the diagonal dynamics of advertisement in Figure 3B.

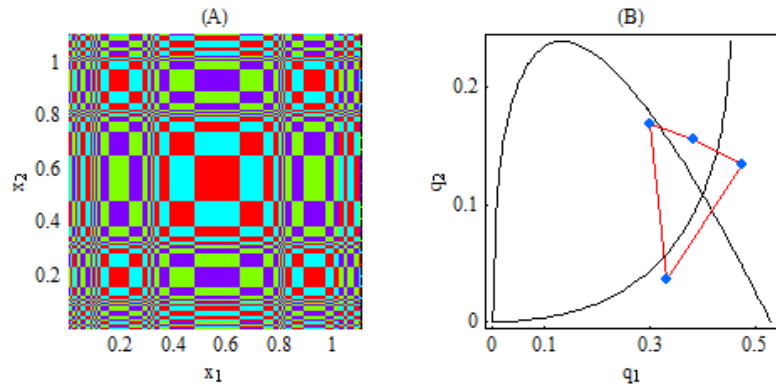


Figure 3. Four basins of attractors with  $a = 3.12$  and a period-4 cycle of output

As  $a$  increases further, we can have more complicated and exotic basins of attractions. It can be checked that  $m$  period- $m$  cycles coexist if  $\varphi(x)$

generates a period- $m$  cycle. One cycle is in the diagonal and the remaining  $(m-1)$  cycles are in the off-diagonal. It can be supposed that the rectangular regions of the basin will be divided further. At the edge of chaos in which  $a$  is at the accumulation point, Shin (2007) mathematically shows how the patterns of those basin structures are composed.

#### 4.1.2 Restricted Homogenous 4D Model

To characterize the dynamics, we restrict our attentions to the behavior in the diagonal, since qualitative features of the off-diagonal dynamics is the same as that of the diagonal dynamics. If the firms start with the symmetric initial point,  $x_1(0) = x_2(0)$ , then advertisements remain equal for all  $t \geq 0$ , i.e.,  $x_1(t) = x_2(t)$ . The double logistic map may be interpreted as a simple logistic map, since the evolution of the advertisement reflects the common behavior of the two firms. In this case, we can write  $x_1 = x_2 = x$  and then the 4D dynamic system can be reduced to the 3D dynamic system,<sup>4</sup>

$$\begin{aligned} q_1' &= \phi_1(q_2, x), \\ q_2' &= \phi_2(q_1, x), \\ x' &= \varphi(x). \end{aligned} \tag{10}$$

In order to determine the confinement condition of the output dynamics, we will distinguish between two cases depending on whether the advertisement dynamics is stable or not, .

If the advertisement model is stable, then its trajectory eventually converges to the stationary point. Thus it is safe to assume that the advertisement evolution starts at its stationary value and stays there afterward. Consequently, the confinement boundary of the output can be obtained by substituting  $x^e$  into  $x_1$  and  $x_2$  of (7),

$$c = \frac{(4 + (1 + x^e)^2)^2}{4(1 + x^e)^3}. \tag{11}$$

If the advertisement model is unstable, then the trajectory may oscillate ranging from the maximum value  $x^{\max}$  of  $\varphi(x)$  to the zero minimum value. The most restrictive confinement constraint on the output dynamics is given by substituting  $x^{\max}$  into  $x_1$  and  $x_2$  of (7),

$$c = \frac{(4 + (1 + x^{\max})^2)^2}{4(1 + x^{\max})^3} \text{ with } x^{\max} = \frac{(1 + a - r)^2}{4a}. \tag{12}$$

---

<sup>4</sup>We denote the eigenvalue of  $\varphi$  by  $\lambda_3$  for convenience.

For the time being we call this relation the confinement condition of the output when the advertisement is unstable. It should be noted, however, that the condition may be violated if an unstable trajectory of the advertisement map takes its maximum value less than  $x^{\max}$ . This could happen if the trajectory is periodic and  $x^{\max}$  is not a periodic point. In spite of this comment, it can be used only as a rough estimate of the confinement condition.

The Hopf and flip boundaries divide the parameter region into stable and unstable regions while the confinement boundaries divide it into feasible and infeasible regions. The 3D system contains three parameters,  $r$ ,  $a$  and  $c$ . Taking  $r$  given, we characterize the stability of the stationary point for the values of parameters  $c$  and  $a$  in the set,

$$D = \{(c, a) \mid 1 \leq c \leq \frac{25}{4}, r \leq a \leq 3 + r\},$$

in which, as will be seen soon,  $\frac{25}{4}$  is the maximum upper bound of the marginal cost ratio for feasible solutions.

Depending on the parametric configuration of  $(c, a)$  in  $D$ , the following cases should be considered:

**(1)**  $a = r$

This condition means the restriction of the 3D dynamic system to the lower boundary of  $D$  and implies that  $x^e = 0$  so no advertisement takes place. The 3D system is further reduced to a 2D system, namely, the output model without advertisement, which is equivalent to Puu's duopoly model. Therefore, the time evolution of the outputs coincides with that of Puu's model. In fact, it can be checked that  $\alpha = \frac{1}{c}$  when  $a = r$ . Thus solving the Hopf bifurcation condition  $(c^{-1} - 1)(c - 1) = -4$  for  $c$  gives the solution  $c_u = 3 + 2\sqrt{2}$  as  $c \geq 1$  is assumed. The Hopf boundary crosses the horizontal line  $a = r$  at  $(3 + 2\sqrt{2}, r)$ . Therefore the stationary state is stable for  $c < c_u$  and becomes unstable for  $c \geq c_u$ . Substituting  $x^e = 0$  into the confinement condition gives the upper bound of the marginal cost ratio,  $\bar{c} = \frac{25}{4}$ . The confinement boundary (11) crosses the horizontal line at  $(\frac{25}{4}, r)$ . As  $c$  increases from  $c_u$ , the stationary point loses its stability, bifurcates to periodic cycles and then exhibits chaotic oscillations for sufficiently higher value of  $c$ . Note that  $c$  cannot be greater than the critical value  $\bar{c}$ , beyond which the model becomes infeasible. These results are the same as those already shown in Puu (2003).

**(2)**  $r < a < 2 + r$

This subset of  $D$  is further divided into two parts by the Hopf boundary,  $(\alpha^{-1} - d)(\alpha - d) = -4$ . In the left side of the boundary in which  $(\alpha^{-1} - d)(\alpha - d) > -4$ ,  $|\lambda_i| < 1$  for  $i = 1, 2, 3$  so the output model as well as the advertisement map are locally stable. In the right side in which  $(\alpha^{-1} - d)(\alpha - d) < -4$ ,  $|\lambda_i| > 1$  for  $i = 1, 2$  and  $|\lambda_3| < 1$ . Thus the output model becomes locally unstable but the advertisement map is still locally stable. The unstable trajectories are bounded by the confinement boundary that is defined by (11),

$$\psi(x^e, x^e) = \frac{(4 + (1 + x^e)^2)^2}{4(1 + x^e)^3}.$$

For dynamic considerations, we assume that advertisement is at its stationary value since the advertisement map is stable. The output model with constant advertisement is linearly conjugate to the output model with zero advertisement, which case is already discussed above.

Figure 4 presents two bifurcation diagrams with respect to  $c$  and  $a$ . The 3D system is iterated 5,000 times to eliminate transient behavior and the last 50 iterated points are plotted. In Figure 4A,  $c$  ranges from 1 to  $\frac{25}{4}$  and  $a$  from  $r$  to  $2 + r$  where  $r = 0.6$  is fixed. Figure 4B is an enlargement of a part of Figure 4A, in which  $c$  ranges from 2.9 to 3.0 and  $a$  from 1.03 to 1.19. Different colors indicate different periods of periodic cycles up to period 16. Periodic points with a larger period than 16 or aperiodic points are colored in grey. Trajectories are infeasible in the white region in which the confinement condition is violated. Red regions in Figures 4A and 4B represent the region where the 3D system is locally stable. The same color in the entire region indicates that any trajectory converges to the stationary point, which, in turn, imply global stability of the 3D system. For  $(c, a)$  crossing the Hopf boundary but not reaching the confinement boundary, the stationary point  $(q_1^e, q_2^e)$  of the output model becomes unstable and generates essentially the same time evolutions as the ones obtained in case (1), which indicates that the stationary point goes to chaos via Hopf bifurcation. In case (1), the emergence of complex dynamics is associated with a highly asymmetric cost structure (i.e.,  $(3 + 2\sqrt{2})c_1 < c_2 < 6.25c_1$ ). In contrast, the same bifurcation scenario takes place in case (2) under more plausible cost structure if the

advertisement outlay is higher, as observed in Figure 4B.

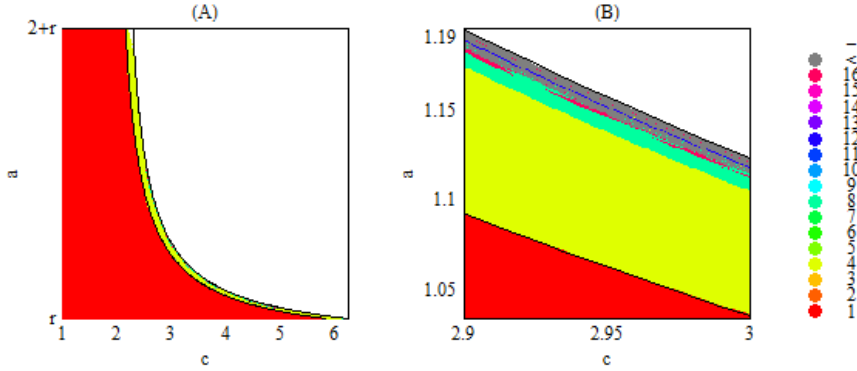


Figure 4. Bifurcation diagram in the  $(c, a)$  space

**(3)**  $2 + r \leq a \leq 3 + r$

In this case  $|\lambda_3| > 1$  always, so the advertisement map is unstable. The output model is unstable if  $(\alpha^{-1} - d)(\alpha - d) > -4$  (that is,  $|\lambda_i| > 1$  for  $i = 1, 2$ ). Moreover, since the advertisement map plays the dominant role for characterizing the dynamics of the output, the output model becomes unstable even if  $(\alpha^{-1} - d)(\alpha - d) \leq -4$ . Figure 5 depicts the two-dimensional bifurcation diagram of (9) in the  $(c, a)$  plane in which  $c$  ranges from 1.8 to 2.3 and  $a$  from  $2 + r$  to  $3 + r$ . As in Figure 4, the regions of periodic and aperiodic behavior are indicated with different colors and the solutions are infeasible in the white region. The negative sloping real line is the Hopf boundary. It can be observed that nothing particular changes if the parameter configuration  $(c, a)$  crosses the Hopf boundary. The negative sloping dotted line is the confinement boundary. Four interesting facts should be mentioned. First, the confinement condition is satisfied for large values of  $a$  as chaos is born for higher values and its trapping interval includes  $x^{\max}$ . Second, this is not the case for smaller values of  $a$ , since only periodic cycles are born and  $x^{\max}$  is not a periodic point. Third, there are some higher values of  $a$  for which windows of chaos emerge with periodic points violating the confinement condition. Finally, there are no differences in dynamics whether the parameter configuration  $(c, a)$  is located in the left or right side of the Hopf boundary, which shows sharp contrast to the result obtained in case (2).

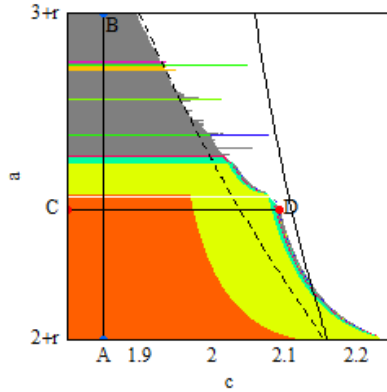


Figure 5. Bifurcation diagram in  $(c, a)$

Parameters  $a$  (as well as  $r$ ) and  $c$  can be thought as the sources of nonlinearities of the advertisement model and the output model, respectively. The larger the parameter is, the stronger the nonlinearities of those models are. The effect caused by a change in  $a$  on output dynamics is however qualitatively different from the effect caused by a change in  $c$ . To see the differences, we first choose  $a$  as the bifurcation parameter and keep  $c$  fixed. Since the advertisement map is qualitatively the same as the logistic map, it exhibits the well-known period-doubling bifurcation after  $a$  crosses the flip boundary (i.e.,  $2 + r$ ) if we increase it to its upper bound,  $3 + r$ . The time evolution of the output is synchronized with that of the advertisement and thus exhibits the period-doubling sequence of bifurcations with respect to  $a$  as shown in Figure 6. Two simulations are performed with different values of  $c$  there. In the first simulation,  $a$  is increased along the vertical segment  $AB$  of Figure 5 while  $c = 1.85$  and  $r = 0.6$  are fixed. The resultant bifurcation diagram against  $a$  is depicted in Figure 6A. In the second simulation, only  $c$  is changed to 1.5 (which value is outside the range of Figure 6 so that it is not illustrated there) and the resultant bifurcation diagram is presented in Figure 6B. The similarity between these two diagrams is clear. Bifurcation occurs for exactly the same values of  $a$ , namely, period-2 cycle bifurcates to period-4 cycle for  $a = a_4$ , which, in turn, bifurcates to period-8 cycle for  $a = a_8$ , further, the window opens for  $a = a_3$  and so on. Differences can also be observed: the range of  $q_1$  as well as the diameter of one of the period-2 cycles become much smaller as  $c$  decreases with all other parameter values kept unchanged.

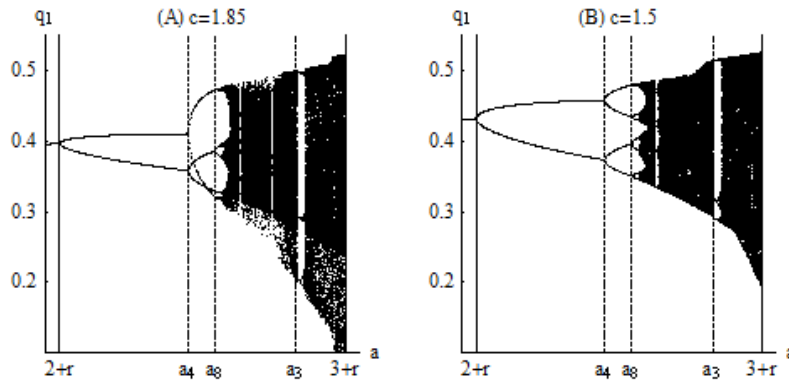


Figure 6. Period-doubling bifurcation diagrams against  $a$

Alternatively, if we choose  $c$  as the bifurcation parameter and fix  $a = 3$  and  $r = 0.6$ , then we have a different type of bifurcation scenario as illustrated in Figure 7 in which we increase  $c$  along the horizontal segment  $CD$  from 1.8 to 2.0935 as shown in Figure 5. Since  $a$  is unchanged along this segment, the advertisement map keeps generating a two period cycle. As shown in Figure 7, a period-2 cycle of the output appears first, which is synchronized with the advertisement evolution. For a larger value of  $c$  (i.e., larger than about 1.97), a period-3 cycle is born because one of the two periodic points bifurcates to a period-2 cycle. As  $c$  increases further, the periodic cycle goes to chaos after repeating many period doubling bifurcations. At the first glance, the well-known bifurcations scenario seems to occur. However, careful observations reveal, as shown below, that the whole model undergoes different type of period-adding bifurcations.

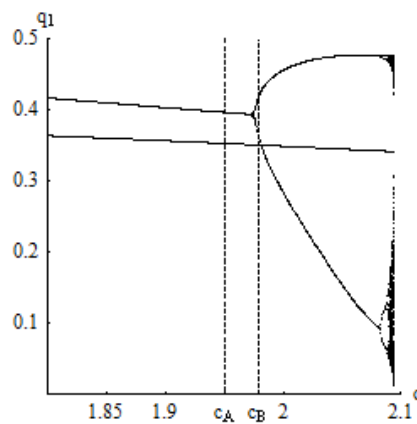


Figure 7. Period-adding bifurcation diagram against  $c$

### 4.1.3 Half-Pitchfork Bifurcation

We now consider the pitchfork bifurcation scenario of the restricted dynamic system (10). To simplify the discussion, we specify the parameter values as  $a = 3$  and  $r = 0.6$  and select the case in which the advertisement model  $\varphi(x)$  generates a period-2 cycle, the lowest-order cycle.<sup>5</sup> Let  $x_1$  and  $x_2$  be the periodic points of the cycle, which are obtained by solving equation  $\varphi(\varphi(x)) = x$ :

$$x_1 = \frac{2 + a - r - \sqrt{(a - r)^2 - 4}}{2a},$$

and

$$x_2 = \frac{2 + a - r + \sqrt{(a - r)^2 - 4}}{2a}.$$

Apparently these points are defined only for  $a > 2 + r$ . We have  $x_1 = 0.51225$  and  $x_2 = 0.95442$ . Let  $x_2$  be an initial point ( $t = 0$ ) of the advertisement map. Then  $x(t)$  oscillates between these two points:  $x_1 = \varphi(x(t))$  if  $t$  is odd and  $x_2 = \varphi(x(t))$  if  $t$  is even. It is thus convenient to re-define the output generating functions as follows: when  $t$  is odd and  $x_1$  is fixed,

$$f_1(q_2, x_1) = (1 + x_1) \left( \sqrt{\frac{q_2}{c_1}} - q_2 \right),$$

$$f_2(q_1, x_1) = (1 + x_1) \left( \sqrt{\frac{q_1}{c_2}} - q_1 \right),$$

and when  $t$  is even and  $x_2$  is fixed,

$$g_1(q_2, x_2) = (1 + x_2) \left( \sqrt{\frac{q_2}{c_1}} - q_2 \right),$$

$$g_2(q_1, x_2) = (1 + x_2) \left( \sqrt{\frac{q_1}{c_2}} - q_1 \right),$$

in which  $x_1$  and  $x_2$  are determined solely by  $a$  and  $r$  and thus they can be treated as positive constants when we consider output dynamics. To find the period-2 points of the output, we define the two-fold iterates as follows:

$$F_{12}^2(q_1) = g_1(f_2(q_1, x_1), x_2) \text{ and } G_{12}^2(q_2) = g_2(f_1(q_2, x_1), x_2),$$

---

<sup>5</sup>We obtain qualitatively the same result even in cases when  $\varphi(x)$  generates higher order cycles and another values of the parameters are specified.

and

$$F_{21}^2(q_1) = f_1(g_2(q_1, x_2), x_1) \text{ and } G_{21}^2(q_2) = f_2(g_1(q_2, x_2), x_1),$$

where the subscripts "ij" mean that the time evolution of the advertisement moves from  $x_i$  to  $x_j$ , and the superscript "2" means that functions are twice folded.

Let us select  $c_A = 1.95$  for which a period-2 cycle of output appears as shown in Figure 7. The vertical dotted line at  $c = c_A$  crosses the two downward sloping curves. Two intersections are the  $q_2$ -periodic points of the period-2 cycle. Solving each of the four equations,  $F_{12}^2(q_1) = q_1$ ,  $G_{12}^2(q_2) = q_2$ ,  $F_{21}^2(q_1) = q_1$  and  $G_{21}^2(q_2) = q_2$ , yields two periodic points of the output dynamic system,

$$Q^A = (q_1^A, q_2^A) \text{ and } Q^B = (q_1^B, q_2^B),$$

where

$$q_1^A = 0.35439, q_2^A = 0.08119, q_1^B = 0.39821 \text{ and } q_2^B = 0.14056.$$

Differentiating each of the two-folded functions gives the following derivative values at the corresponding periodic points:

$$F_{21}^{2'}(q_1^A) = G_{12}^{2'}(q_2^B) = -0.39301 \text{ and } G_{21}^{2'}(q_2^A) = F_{12}^{2'}(q_1^B) = -0.96651.$$

All derivatives are less than unity in absolute value so this period-2 cycle is stable and thus, any trajectory starting at any point of the feasible region is asymptotically periodic to the period-2 cycle.

Next, fixing the values of  $a$  and  $r$ , we increase the value of  $c$  to  $c_B = 1.97725$ . Since  $a$  and  $r$  remain unchanged, the advertisement map still generates the period-2 cycle,  $x_1$  and  $x_2$ , while the change in  $c$  induces qualitative changes in the output dynamics. The output model now seems to give rise to a period-3 cycle according to the bifurcation diagram of Figure 7 in which the vertical dotted line intersects three times with the curves depicted. However, in fact, it generates a period-4 cycle as will be seen shortly. To show the emergence of the period-4 cycle, it is convenient to introduce the following four-fold iterates:

$$F_{12}^4(q_1) = F_{12}^2(F_{12}^2(q_1)) \text{ and } G_{12}^4(q_2) = G_{12}^2(G_{12}^2(q_2)),$$

and

$$F_{21}^4(q_1) = F_{21}^2(F_{21}^2(q_1)) \text{ and } G_{21}^4(q_2) = G_{21}^2(G_{21}^2(q_2)).$$

The same principle is used for defining the subscripts and superscripts of these functions as before. The fixed points of these four-folded functions are

composed of the periodic points of the period-4 cycle, which are denoted by  $A, B, C$  and  $D$  in Figure 6. The fixed points are calculated as given below, where the superscript indicates an element of the corresponding periodic points:

$$\begin{aligned} F_{21}^4(q_1) = q_1 &\implies q_1^B = q_1^D = 0.350469 \\ G_{21}^4(q_2) = q_2 &\implies q_2^B = 0.06613 \text{ and } q_2^D = 0.09524, \\ F_I^4(q_1) = q_1 &\implies q_1^A = 0.41266 \text{ and } q_1^C = 0.37336, \end{aligned}$$

and

$$G_{12}^4(q_2) = q_2 \implies q_2^A = q_2^C = 0.13647.$$

Derivatives of these functions at the fixed points are also calculated as

$$F_{12}^{4'} = G_{21}^{4'} = 0.99266 \text{ and } F_{21}^{4'} = G_{12}^{4'} = 0.17544.$$

All of these values are less than unity in absolute value so the period-4 cycle is stable and any trajectory is asymptotically periodic to it. Fixing the parameter values of the advertisement map and increasing the marginal cost ratio of the output model result in a bifurcation of the period-2 cycle to period-4 cycle. The question that we naturally raise is how such a bifurcation develops.

To understand the birth of the period-4 cycle, consider, first, the two-folded functions  $F_{ij}^2$  and  $G_{ij}^2$  for  $i, j = 1, 2$  and  $i \neq j$  with  $c = c_B$ . Following the same procedure we have done above, we can obtain a period-2 cycle whose periodic points are depicted as two red points,  $a$  and  $b$ , in the first quadrant of Figure 8. Two red points in the second and fourth quadrants correspond to periodic points in the output-advertisement plane. However this period-2 cycle is unstable. To show this fact, we solve  $F_{ij}^2(q_1) = q_1$  and  $G_{ij}^2(q_2) = q_2$  to obtain the periodic points,

$$q_1^a = 0.39462, \quad q_2^a = 0.13647 \text{ and } q_1^b = 0.35227, \quad q_2^b = 0.07881,$$

and then differentiate the functions at the fixed points to obtain the derivatives

$$F_{12}^{2'}(q_1^a) = G_{21}^{2'}(q_2^b) = -1.00183 \text{ and } F_{21}^{2'}(q_1^b) = G_{12}^{2'}(q_2^a) = -0.41886.$$

These results lead to the following conclusion. At point  $a$ ,  $q_1^a$  is unstable while  $q_2^a$  is stable. On the other hand, at point  $b$ ,  $q_1^b$  is stable while  $q_2^b$  is unstable. The period-2 cycle with  $c = c_B$ , therefore, becomes one half stable and the other half unstable.

It is evident that these unstable fixed points of  $F_{12}^2(q_1)$  and  $G_{21}^2(q_2)$  are also the fixed points of  $F_{12}^4(q_1)$  and  $G_{21}^4(q_2)$ . Moreover since  $F_{12}^{4'}(q_1^a) =$

$(F_{12}^{2'}(q_1^a))^2 > 1$  and  $G_{21}^{4'}(q_2^b) = (G_{21}^{2'}(q_2^b))^2 > 1$ ,  $q_1^a$  and  $q_2^b$  are repelling. As done above, equations  $F_{12}^4(q_1) = q_1$  and  $G_{21}^4(q_2) = q_2$  provide two additional stable fixed points, which are illustrated in Figure 8 as the blue points. In the fourth quadrant, which corresponds to the  $(q_1, x)$  plane, there are two blue dots and one red dot for  $x_1$ ;  $q_1^A$  and  $q_1^C$  are shown by the blue dots and  $q_1^a$  is shown by the red dot. This picture indicates that in the case when the eigenvalue of  $F_{12}^2(q_1)$  equals  $-1$ , the stability of the period-2 cycle is in this case just lost and at the same time, two new fixed points of  $F_{12}^4(q_1)$  are born. This phenomenon, as well-known, is called the period doubling bifurcation. However, the fixed point of  $F_{21}^4(q_1)$  does not bifurcate as far as the advertisement map gives rise to the period-2 cycle. In the second quadrant, which corresponds to the  $(x, q_2)$  plane, there are also two blue dots and one red dot. The same phenomenon is occurred in  $G_{21}^2$  and  $G_{21}^4$  so at  $c$ , for which  $G_{21}^{2'}(q_2^b) = -1$ ,  $G_{21}^2$  becomes unstable and  $G_{21}^4$  undertakes a period-doubling bifurcation and two new fixed points of  $G_{21}^2$  are created.

We can summarize the above results as follows. The period-2 cycle is attracting for  $c = c_A$  but becomes repelling for  $c = c_B$ .  $F_I^4(q_1)$  does not have a period-4 cycle for  $c = c_A$  but it has an attracting period-4 cycle of output for  $c = c_B$ . There is a critical value of  $c$  between these two values, at which the eigenvalues of the two-fold iterate are equal to  $-1$ , and those of the four-iterates equal 1.<sup>6</sup> The bifurcation from period-2 cycle to period-4 cycle takes place just at this critical value.

---

<sup>6</sup>We encountered difficulties when we tried to derive a general expression of this critical value without specifying the values of  $a$  and  $r$ , since, we needed to solve a cubic equation whose solution may have very complicated expression in general.

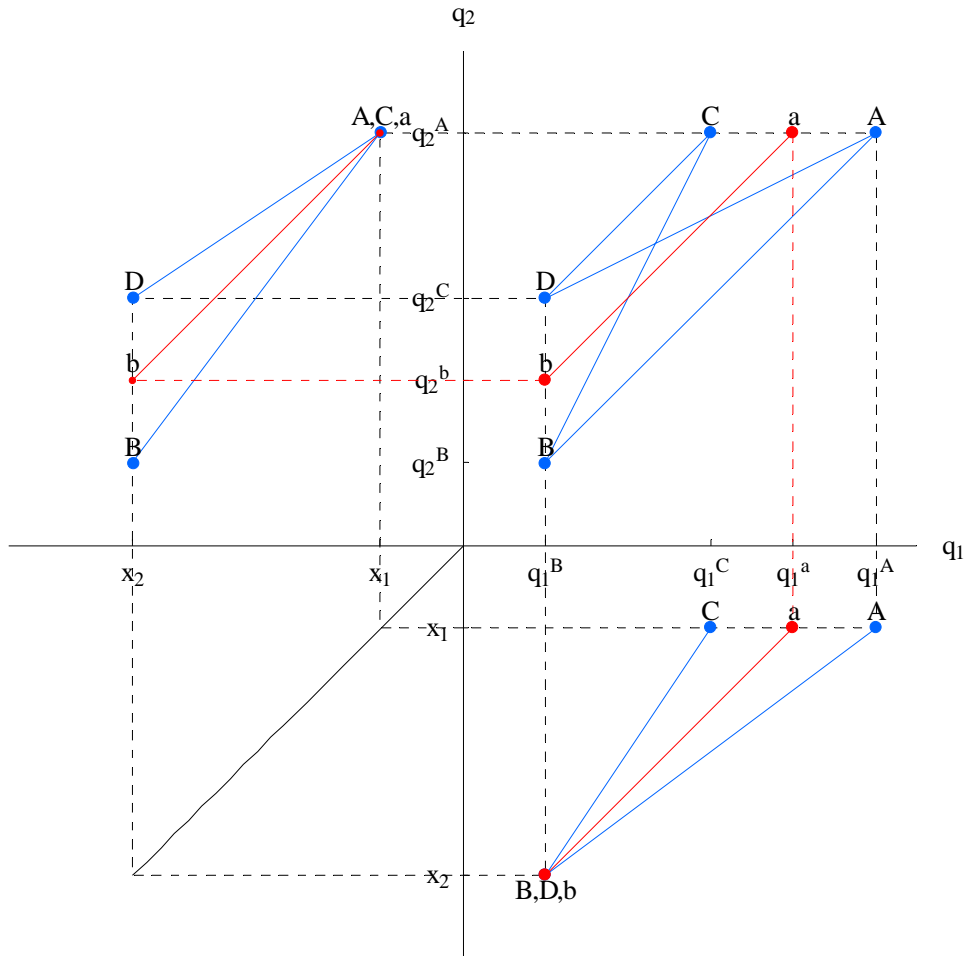


Figure 8. Birth of period-4 cycle from period-2 cycle.

As  $c$  increases further, additional bifurcation occurs and new fixed points are created repeatedly in the same way as just described. A sequence of this type of bifurcation leads to complicated dynamics. Notice however that even if aperiodic cycle of the output emerges, the advertisement trajectory still oscillates between two points  $x_1$  and  $x_2$  since its dynamics is independent of the value of  $c$ . In Figure 9, two different attractors are illustrated: on the left side,  $c = 2.093$  and  $(a, r) = (3, 0.6)$  for which the advertisement map gives rise to the period-2 cycle and on the right side,  $c = 1.9$  and  $(a, r) = (3.5, 0.6)$  for which the advertisement map gives rise to chaotic behavior, therefore the output also behaves chaotically.

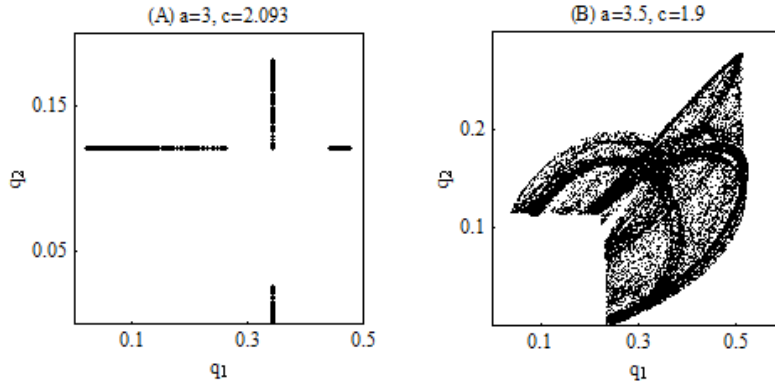


Figure 9. Two attractors with different values of  $a$

## 4.2 Heterogeneous Advertisement

In this section we remove the simplifying assumption of homogeneity and return to the original 4D dynamic model (1) that is composed of the output dynamic model,  $q'_i = \phi_i(q_j, x_i)$ , and the advertisement dynamic model,  $x'_i = \varphi_i(x_i)$  for  $i, j = 1, 2$ . As shown in Lemmas 1 and 2, there are three ways to violate the local stability conditions: a set of parameters crosses one of the flip boundaries  $a_1 = 2 + r_1$ ,  $a_2 = 2 + r_2$  or the Hopf boundary  $(\alpha^{-1} - d_1)(\alpha - d_2) = -4$ . Since the time-evolution of the stationary point depends on the values of  $r_i, a_i$  and  $c$ , we consider dynamic characterization in the parametric region  $A$  defined above by changing the value of  $c$  with fixed values of  $r_1$  and  $r_2$  at 0.6.<sup>7</sup> Each of the two flip boundaries and the Hopf boundary divides  $A$  into two subsets; the stable region in which the absolute value of the corresponding eigenvalue is less than unity and the unstable region in which  $|\lambda_i| > 1$ . Thus, set  $A$  can be divided into  $2^3$  parts because there are essentially three eigenvalues and each of them can be greater or less than unity in absolute value.<sup>8</sup> The actual number of the division depends on the value of  $c$ , the parameter controlling the nonlinearity of the output model. In the first case, the division of  $A$  by the two flip boundaries is examined:

$$\begin{aligned}
 A_{SS} &= \{(a_1, a_2) \in A \mid r_1 \leq a_1 < 2 + r_1 \text{ and } r_2 \leq a_2 < 2 + r_2\}, \\
 A_{SU} &= \{(a_1, a_2) \in A \mid 2 + r_1 \leq a_1 \leq 3 + r_1 \text{ and } r_2 \leq a_2 < 2 + r_2\}, \\
 A_{US} &= \{(a_1, a_2) \in A \mid r_1 \leq a_1 < 2 + r_1 \text{ and } 2 + r_2 \leq a_2 \leq 3 + r_2\}, \\
 A_{UU} &= \{(a_1, a_2) \in A \mid 2 + r_1 \leq a_1 \leq 3 + r_1 \text{ and } 2 + r_2 \leq a_2 \leq 3 + r_2\},
 \end{aligned}$$

<sup>7</sup>Needless to say, a choice of the particular values of  $r_i$  does not affect the qualitative aspects of the results obtained below.

<sup>8</sup>Although there are actually four eigenvalues, it is sufficient to consider the division of  $A$  by only three of them, since  $\lambda_1 = -\lambda_2$  with identical absolute values.

where the first (respectively, the second) subscript of  $A$  denotes  $S$  or  $U$  according to whether the stationary point of firm 1's (respectively, firm 2's) advertisement is stable or unstable. The first question we are concerned is how the value of  $c$  further divides  $A$ .

To answer this question, let us begin our analysis by defining three critical values of  $c$  for which the Hopf boundary just passes through the three points,  $(3 + r_1, 3 + r_2)$ ,  $(2 + r_1, 2 + r_2)$ , and  $(r_1, r_2)$ , respectively. Let  $a_i$  be equal to  $k + r_i$  for  $k = 0, 2, 3$ . Considering  $z$  as an unknown, we first solve the Hopf boundary condition,  $-4 = (z^{-1} - d_1)(z - d_2)$  for  $z$ , where  $d_i = 2 - \frac{r_i}{a_i}$  and  $a_i = k + r_i$ . Then we substitute the solution into equation (5) and then solve it for  $c$  to obtain the critical value in terms of  $r_i$  and  $k$ . Taking  $r_i = 0.6$  for  $i = 1, 2$  as given, we obtain the following critical values:

$$c_{k=3} = 2.05865, \quad c_{k=2} = 2.15917 \quad \text{and} \quad c_{k=0} = 5.828\dots (= 3 + 2\sqrt{2}).$$

The value  $3 + 2\sqrt{2}$  is the marginal cost ratio for which Puu's duopoly model loses stability. Therefore  $c_{k=0} = 3 + 2\sqrt{2}$  is intuitively clear because with  $a_i = r_i$ , the model is reduced to Puu's model as seen in case (1) of Section 4.1.2. According to the three critical value of  $c$ , four cases have to be considered.

**(1)**  $c \leq c_{k=3}$

If the marginal cost ratio is small enough, so strict inequality holds, then there is no intercept of the Hopf boundary curve with any part of  $A$ . As a result,  $(\alpha^{-1} - d_1)(\alpha - d_2) > -4$  for all  $(a_1, a_2) \in A$ , so the output model with constant advertisement is stable. Notice that the properties of the advertisement dynamics depend on the choice of  $(a_1, a_2)$  from  $A$ , and the time evolution of the output is affected by the dynamics of the adjustment model. Therefore, the properties of the output dynamics also depend on the choice of  $(a_1, a_2)$  from  $A$ . In particular, for  $(a_1, a_2) \in A_{SS}$ , the advertisement dynamics is stable so is the output dynamics. On the other hand, for  $(a_1, a_2) \in A \setminus A_{SS}$ , the complementary set of  $A_{SS}$ , one or both of the advertisement maps is unstable and so is the output model.

Let us examine the unstable cases in more detail. If  $(a_1, a_2)$  is chosen from either  $A_{SU}$  or  $A_{US}$ , one of the advertisement maps is unstable and the other is stable. Thus we can limit our discussion to dynamics generated by the output model and the unstable advertisement map, because the stable advertisement map does not affect asymptotic behavior of the other variables. To simplify the discussion, the 4D dynamic system can be reduced to a 3D dynamic system whose dynamics is essentially the same as the one generated by (10) where  $\varphi(x)$  is replaced with the unstable advertisement map  $\varphi_i(x_i)$ .

For  $(a_1, a_2) \in A_{UU}$ , both advertisement maps are unstable and produce complex dynamics as  $a_i$  is approaching its upper bound. It is easily expected that the output model generates complex dynamics affected by the complex behavior of the advertisement. It is repeatedly stated that the emergence of complex dynamics is one feature of the output dynamics. It also follows from the discussions of Section 4.1.1 that another feature of the output dynamics is multistability, namely coexistence of stable periodic cycles. Here we turn our attention to this issue and address the following important question: if  $\varphi_1(x)$  and  $\varphi_2(x_2)$  have a stable period- $m$  cycle and a stable period- $n$  cycle, respectively, then how many cycles does the advertisement model generate.

We start with the simple case in which  $\varphi_1(x)$  gives rise to a stable period-2 cycle and  $\varphi_2(x_2)$  a stable period-3 cycle. Let  $X_1 = \{x_1^A, x_1^B\}$  be a set of two periodic points with the eigenvalue  $\lambda_1 = \varphi_1'(x_1^A)\varphi_1'(x_1^B)$  and  $X_2 = \{x_2^A, x_2^B, x_2^C\}$  a set of three periodic points with the eigenvalue  $\lambda_2 = \varphi_2'(x_2^A)\varphi_2'(x_2^B)\varphi_2'(x_2^C)$ . In considering the iteration of the advertisement maps, we first redefine the advertisement dynamics as a two-dimensional map  $\Phi : R^2 \rightarrow R^2$  given by

$$\Phi(x_1, x_2) = (\varphi_1(x_1), \varphi_2(x_2)),$$

and then focus on the  $2 \times 3$  points of the  $(x_1, x_2)$  space obtained by the Cartesian product  $X_1 \times X_2$ . It can be checked that a period-6 cycle is formed by these six points because the least common multiple period of period-2 and period-3 cycles is six,

$$\{\Phi^t(x_1^A, x_2^A), t = 1, \dots, 6\}.$$

The stability of the period-6 cycle can be shown as follows. Denote the iteration of the advertisement map by  $\varphi_i^t(x_i) = \varphi_i(\varphi_i^{t-1}(x_i))$  and  $\varphi_i^0(x_i) = x_i$ . Since  $x_1^A$  is the fixed point of  $\varphi_1^2(x_1)$  and  $x_2^A$  is the fixed point of  $\varphi_2^3(x_2)$ , differentiating the two-dimensional map at the fixed points

$$(x_1^A, x_2^A) = \Phi^6(x_1^A, x_2^A) = (\varphi_1^{2 \times 3}(x_1^A), \varphi_2^{3 \times 2}(x_2^A))$$

yields the Jacobi matrix

$$J(x_1^A, x_2^A) = \begin{pmatrix} (\varphi_1'(x_1^A)\varphi_1'(x_1^A))^3 & 0 \\ 0 & (\varphi_2'(x_2^A)\varphi_2'(x_2^B)\varphi_2'(x_2^C))^2 \end{pmatrix}.$$

The eigenvalues of the period-6 cycle are  $\lambda_1^A = (\lambda_1)^3$  and  $\lambda_2^A = (\lambda_2)^2$  so the period-6 cycle is stable if the original period-2 and the period-3 cycles are stable, that is  $|\lambda_i| < 1$  for  $i = 1, 2$ .

We proceed to the next case in which  $\varphi_1(x)$  gives rise to a period-2 cycle with periodic points  $X_1 = \{x_1^A, x_1^B\}$  and  $\varphi_2(y)$  a period-4 cycle with periodic points  $X_2 = \{x_2^A, x_2^B, x_2^C, x_2^D\}$ . Eigenvalues of the two cycles are  $\lambda_1 = \varphi_1'(x_1^A)\varphi_1'(x_1^B)$  and  $\lambda_2 = \varphi_2'(x_2^A)\varphi_2'(x_2^B)\varphi_2'(x_2^C)\varphi_2'(x_2^D)$ , respectively. Set  $X_1 \times X_2$  has eight points, and since the least common multiple period of period-2 and period-4 cycles is 4, there are  $8/4 = 2$  period-4 cycles:

$$\{\Phi^t(x_1^A, x_2^A), t = 1, \dots, 4\},$$

and

$$\{\Phi^t(x_1^A, x_2^B), t = 1, \dots, 4\}.$$

Since the first period-4 cycle visits its periodic points in the order of  $(x_1^A, x_2^A) \rightarrow (x_1^B, x_2^B) \rightarrow (x_1^A, x_2^C) \rightarrow (x_1^B, x_2^D)$ , the Jacobi matrix is

$$J(x_1^A, x_2^A) = \begin{pmatrix} (\varphi_1'(x_1^A)\varphi_1'(x_1^B))^2 & 0 \\ 0 & \varphi_2'(x_2^A)\varphi_2'(x_2^B)\varphi_2'(x_2^C)\varphi_2'(x_2^D) \end{pmatrix},$$

and by the same way, since the second cycle is formed as  $(x_1^A, x_2^B) \rightarrow (x_1^B, x_2^C) \rightarrow (x_1^A, x_2^D) \rightarrow (x_1^B, x_2^A)$ , its Jacobi matrix is

$$J(x_1^A, x_2^B) = \begin{pmatrix} (\varphi_1'(x_1^A)\varphi_1'(x_1^B))^2 & 0 \\ 0 & \varphi_2'(x_2^B)\varphi_2'(x_2^C)\varphi_2'(x_2^D)\varphi_2'(x_2^A) \end{pmatrix}.$$

The two period-4 cycles have the same eigenvalues,  $\lambda_1 = (\lambda_1)^2$  and  $\lambda_2 = (\lambda_2)^4$  so each period-4 cycle is stable if the original period-2 cycle and the period-4 cycle are stable.

Now we move to the general case in which  $\varphi_1(x_1)$  gives rise to a period- $m$  cycle with periodic points  $X_1 = \{x_1^1, x_1^2, \dots, x_1^m\}$  and  $\varphi_2(x_2)$  a period- $n$  cycle with periodic points  $X_2 = \{x_2^1, x_2^2, \dots, x_2^n\}$ . The least common period of period- $m$  and period- $n$  cycles is the least common multiple,  $q$ , of  $m$  and  $n$ , and there are  $mn$  points in  $X_1 \times X_2$ . Let  $k = mn/q$ , then this formula implies that the  $mn$  points obtained by the Cartesian product  $X_1 \times X_2$  can be divided into  $k$  subsets, each of which consists of  $q$  points:

$$\{\Phi^t(x_1^\alpha, x_2^\alpha) = (\varphi_1^t(x_1^\alpha), \varphi_2^t(x_2^\alpha)), t = 1, \dots, q\} \text{ for } \alpha = 1, \dots, k,$$

so we have  $k$  period- $q$  cycles. The stability of the period- $q$  cycle is determined by the eigenvalues of  $\varphi_i^t(x_i)$ ,  $\lambda_1 = \prod_{i=1}^q \varphi_1'(x_1^i)$  and  $\lambda_2 = \prod_{i=1}^q \varphi_2'(x_2^i)$ . Then any period- $q$  cycle is stable if the original periodic cycles are stable. We summarize these results as follows:

**Theorem 3** *Suppose that  $\varphi_i(x_i)$  has a period- $m$  cycle,  $\varphi_j(x_j)$  has a period- $n$  cycle and  $q$  is the least common multiple of  $m$  and  $n$ . Let  $k = mn/q$ . Then the advertisement model generates  $k$  coexisting period- $q$  cycles and each period- $q$  cycle is stable if both of the period- $m$  cycle and the period- $n$  cycle are stable.*

(2)  $c_{k=3} < c \leq c_{k=2}$

If  $c > c_{k=3}$ , then the Hopf boundary crosses some part of  $A$  so that  $A$  is further divided. From an economic point of view, the output must be non-negative and thus must satisfy the confinement conditions  $c \leq \psi(x_1, x_2)$  where  $\psi$  is defined in (8). In Figure 10A in which  $c = 2.075$ , three downward sloping curves are depicted in  $A_{UU} \cup A_{SU}$ . The right most curve is the Hopf boundary, the curve depicted in  $A_{UU}$  is the confinement boundary to be defined in the case where both advertisement stationary points,  $x_1^e$  and  $x_2^e$ , are unstable and the curve illustrated in  $A_{SU}$  is the confinement boundary to be defined in the case where  $x_1^e$  is unstable but  $x_2^e$  is stable. The confinement boundary depicted in  $A_{UU}$  is defined by  $c = \psi(x_1^{\max}, x_2^{\max})$  where

$$x_i^{\max} = \frac{(1 + a_i - r_i)^2}{4a_i} \text{ for } i = 1, 2.$$

For  $(a_1, a_2) \in A_{UU}$ ,  $\varphi_i(x_i)$  may be chaotic so it may take its maximum value, denoted by  $x_i^{\max}$  along the chaotic trajectory. To prevent output from becoming negative, we require the most strict confinement constraint when  $\varphi(x_i)$  is unstable. The confinement boundary depicted in  $A_{US}$  is defined by  $c = \psi(x_1^{\max}, x_2^e)$ , since  $x_1^e$  is unstable and  $x_2^e$  is stable. In the same way,  $c = \psi(x_1^e, x_2^{\max})$  can be defined as the confinement boundary in  $A_{SU}$  in which  $x_1^e$  is stable but  $x_2^e$  is unstable. It is not shown in Figure 10A, since this confinement curve does not intersect with  $A_{SU}$  so it is ineffective. One or both confinement conditions are violated in the white region. The output model is stable in the left side of the Hopf boundary and unstable in the right side. The whole system is stable in  $A_{SS}$ . Dynamics in  $A_{SU}$  and in the feasible (i.e., colored) region of  $A_{US}$  is described by the 3D system obtained by eliminating the stable advertisement map from the 4D system. The dynamics in the feasible region of  $A_{UU}$  is qualitatively the same as the one considered in case (1) just above.

(3)  $c_{k=2} < c \leq c_{k=0}$

We set  $c = 2.35$  in Figure 10(B) where four downward sloping curves are depicted. The most left curve is the Hopf boundary. Three other downward

sloping curves give the confinement boundaries,  $c = \psi(x_1^e, x_2^{\max})$  in  $A_{SU}$ ,  $c = \psi(x_1^e, x_2^e)$  in  $A_{SS}$  and  $c = \psi(x_1^{\max}, x_2^e)$  in  $A_{SU}$ , respectively. The white region that includes the entire  $A_{UU}$  is infeasible. It can be seen that an increase in the value of  $c$  shifts the Hopf boundary and the confinement boundaries leftward. Two further observations emerge by comparing Figure 10(A) with Figure 10(B): (1) the effect on the Hopf boundary is so strong that it shifts the boundary from the right most line to the left most line and (2) the  $c = \psi(x_1^e, x_2^{\max})$  curve divides  $A_{US}$  and thus the output trajectories become infeasible (i.e., negative) for some configurations of  $(a_1, a_2)$ . Dynamics in the feasible regions is governed by a 3D or 2D system according to which equation is stable or unstable.

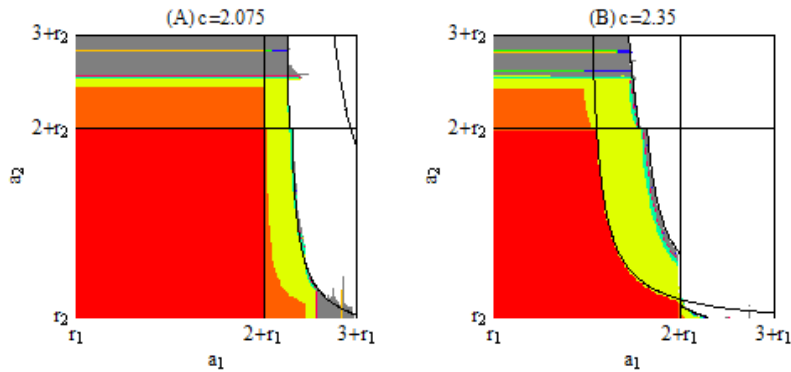


Figure 10. 2-parameter bifurcation diagrams with different values of  $c$

We now turn our attentions to the dynamics in  $A_{SS}$  in order to consider multistability due to nonlinearities of the output model. In  $A_{SS}$  between the Hopf boundary and the confinement boundary  $c = \psi(x_1^e, x_2^e)$ , the advertisement model is stable while the output model is unstable but may be feasible. Thus in the following, we limit our analysis to the case in which the advertisement adjustment is so rapid that the asymptotic output dynamics can be considered to be governed by the iteration of the two-dimensional map

$$\begin{aligned} q_1' &= \phi_1(q_2, x_1^e), \\ q_2' &= \phi_2(q_1, x_2^e). \end{aligned} \tag{3'}$$

This is the special case of the output model (3) in which the advertisement takes its stationary value.<sup>9</sup> It is the topological conjugate of Puu's nonlinear

<sup>9</sup>The very special model with  $x_1^e = x_2^e$  has already been considered in case (2) of Section 4.1.2.

duopoly model. Puu (2003) has already demonstrated that this model with naive and adaptive expectations can give rise to not only rich dynamics ranging from periodic behavior to chaotic dynamics but also to the coexistence of attracting sets by applying the results of Bischi, Mammana and Gardini (2001) and Agliar, Bischi and Gardini (2002). Therefore multistability can be a characteristic property of the output model (3'). It should be noted that output trajectories could be negative on the way to the attractor if the convergence of the stable advertisement dynamics is supposed to be sluggish. As will be suggested later, we need to take the nonnegativity constraint into account in the best response behavior in this case.

(4)  $c_{k=0} < c$

In Figure 12, we set  $c = 3 + 2\sqrt{2}$  for which the Hopf boundary curve passes through the point  $(r_1, r_2)$ . We have  $|\lambda_i| > 1$  in  $A$  for  $i = 1, 2$ , but the solutions for the output are feasible only inside of the triangular region surrounded by the confinement boundary,  $c = \psi(x_1^e, x_2^e)$ . It can be seen that the periodic cycles double their periods as the pair  $(a_1, a_2)$  moves toward the upper bound. In Puu's model, the marginal cost ratio  $c$  is the source of nonlinear dynamics. Introducing the advertisement into Puu's model shows that advertisement outlays also can be the source.

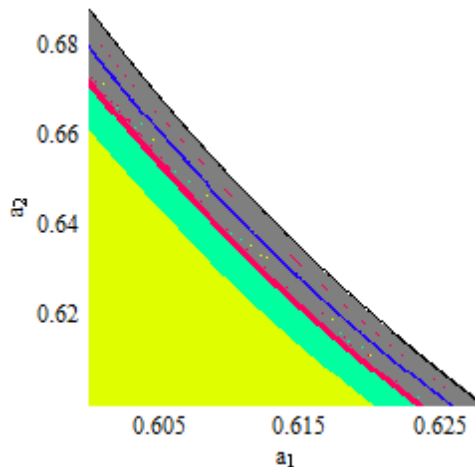


Figure 11 2-parameter bifurcation diagram with  $c = 3 + 2\sqrt{2}$ .

## 5 Conclusion

The present study considers local as well as global dynamics in nonlinear duopoly models with advertisement, which consist of two submodels, the

output dynamic model and the advertisement dynamic model. It first determines the stationary state of the model which is the basis of the stability analysis. We show that the model can be destabilized in two ways: one is through destabilizing the advertisement model when the parameter configurations cross over the flip boundary where one of the eigenvalues is  $-1$ . The other is through destabilizing the output model when the parameter configurations cross over the Hopf boundary on which the eigenvalues are pure imaginary and their common absolute value is unity. It demonstrates that a half-pitchfork bifurcation of the output occurs when the advertisement model gives rise to periodic cycle and the nonlinearity of the output model becomes stronger. The explicit treatment of the confinement conditions reveals the appropriate parameter configurations which prevent unstable trajectories from becoming negative. We also demonstrated that the multistability - coexistence of attracting sets - is the distinguished feature of the model.

The present model should be extended at least in two different directions. One direction is to take away Assumption 1, the simplifying assumption on the advertisement. Under the general condition,  $b_i > 0$ , the advertisement model also has the multistability and thus enhances output dynamics. The other direction is to take the nonnegativity condition into account. The feasibility of the output trajectories can also be enforced by modifying the best response mapping of the firm as follows:

$$q'_i = \begin{cases} 0 & \text{if } q_j \geq \frac{1}{c_i}, \\ (1 + x_i) \left( \sqrt{\frac{q_j}{c_i}} - q_j \right) & \text{otherwise.} \end{cases}$$

In this case the best responses are defined as the profit maximizing outputs under the nonnegativity condition. This new method results in different dynamic properties than those discussed in this paper. We will return to this modified model with positive  $b_i$  in a future paper.

## References

- [1] Agliari, A., G-I., Bischi and L. Gardini, "Some Methods for the Global Analysis of Dynamic Games Represented by Iterated Noninvertible Maps," in Puu and Sushko (2002), 31-83, 2002, Springer.
- [2] Ahmed, E., H. N. Agiza and S. Z. Hassan, "On Modeling Advertisement in Cournot Duopoly," *Chaos, Solitons and Fractals*, vol. 10, 1179-1184, 1994.
- [3] Bischi, G-I., C. Chiarella, M. Kopel and F. Szidarovszky, *Nonlinear Oligopolies: Stability and Bifurcations*, to be published in 2008.
- [4] Bischi, G-I., C. Mammama, and L. Gardini, "Multistability and cyclic attractors in duopoly games," *Chaos, Solitons and Fractals*, vol. 11, 543-564, 2000.
- [5] Feichtinger, G., R. F. Hartl and S. P. Sethi, "Dynamic Optimal Control Models in Advertising: Recent Developments," *Management Science*, vol. 40, 195-226, 1994.
- [6] Kopel, M., "Simple and Complex Adjustment Dynamics in Cournot Duopoly Models," *Chaos, Solitons and Fractals*, vol.7, 2031-2048,1996.
- [7] Luhta, I., and I. Virtanen, "Non-linear Advertisement Capital Model with Time Delayed Feedback between Advertising and Stock of Goodwill," *Chaso, Solitons and Fractals*, vol. 7, 2083-2014, 1996.
- [8] Nerlove, M., and K. Arrow, "Optimal Advertising Policy under Dynamic Conditions," *Econometrica*, vol. 29, 129-142, 1962.
- [9] Puu, T., "Chaos in Duopoly Priceing," *Chaos, Solitons and Fractals*, vol.1, 573-581, 1991.
- [10] Puu, T., and I. Sushko, *Oligopoly Dynamics*, Springer, 2002.
- [11] Rand, D., "Exotic Phenomena in Games and Duopoly Models," *Journal of Mathematical Economics*, vol. 5, 173-184. 1978.
- [12] Shin, G-S, "Interwoven Basin Structure of Double Logistic Map at the Edge of Chaos," mimeo, 2007.
- [13] Sethi, S. P., "Dynamic Optimal Control Models in Advertig: A Survey," *SIAM Review*, vol. 19, 685-725, 1977.